Available online at www.sciencedirect.com
SCIENCE DIRECT®
Pattern Recognition 39 (2006) 363–372
PATTERN RECOGNITION
THE JOURNAL OF THE PATTERN RECOGNITION SOCIETY
www.elsevier.com/locate/patcog

Conflating two polygonal lines☆

Sukhamay Kundu*

Computer Science Department, Louisiana State University, Baton Rouge, LA 70803, USA

Received 10 December 2003; received in revised form 8 December 2004; accepted 16 December 2004

Abstract

A basic technique in comparing and detecting changes in geographical spatial data from satellite images consists of identifying linear features or edges in the image and then matching those features. A chain of connected linear features which form a polygonal line is used as the basic unit for matching two images. We develop a distance measure between two polygonal lines and an efficient algorithm for conflating or optimally matching two polygonal lines based on this distance measure. We show that some of the alternative approaches used in the literature, including Hausdorff's distance, fail to satisfy the basic requirements of a distance measure for image conflation.

Keywords: Distance measure; Image conflation

1. Introduction

The general map conflation problem [1–3] consists of integrating different image data-sets, which may have been collected over a period of time using different imaging technologies and thus resulting in different resolution and details. Two major difficulties in image conflation arise from: (1) the differences in preprocessing of the raw image data to simplify the image before conflation, and (2) the differences in the basic image-objects themselves (roads, buildings, vegetation, coast lines) that occur over time due to natural causes or human activities. In particular, a given object in one image may not exactly match any of the objects in the other image. Also, it may be necessary to rotate and translate one image in order to match the objects in the two images. The matching of two objects is based on their geometric features and thus an object is represented by approximating its boundary by a polygonal line following a basic edge-detection step. One then attempts to pair up major objects in one image with those in the other image which have the best matching. The goal is to find a single transformation (rotation and translation) which brings as many major objects as possible in one image close to those in the other image. The conflation problem becomes more difficult when the images do not correspond to the same geographical region, in which case one has to essentially determine the common or "overlapping" part between the two images by using the conflation of a subset of the major objects in the two images.

We focus here on the fundamental problem of finding the transformation for optimal matching of two polygonal lines (in short, polylines). Our main contributions are: (1) A distance measure $D_2(L_1, L_2)$ that can be used as a measure of the quality of a matching and which satisfies a set of five basic requirements for the conflation problem. We also show that some of the alternative approaches proposed in the literature fail to satisfy the basic five requirements. (2) An efficient algorithm for conflating two polylines, i.e., determining the rotation and translation which minimizes the distance between two polylines.

☆ This research is supported by the NGA Grant NMA401-02-1-2006.
* Tel.: +1 2255782246; fax: +1 2255781465.
E-mail address: kundu@bit.csc.lsu.edu.

0031-3203/$30.00
doi:10.1016/j.patcog.2004.12.017

2. Distance measure

Let $P_i = \langle L_{i1}, L_{i2}, \ldots, L_{im}\rangle$, $i=1,2$, denote two polylines each consisting of m linear segments L_{ij}, $1 \leqslant j \leqslant m (= |P_1| = |P_2|)$. If we are given a distance-function $D(L_1, L_2)$ between two line segments, then a simple way of defining a distance $D(P_1, P_2)$ between P_1 and P_2 is by (1.1) below. One can alternatively define $D(P_1, P_2)$ by (1.2) which basically amounts to adding for each P_i the imaginary line segment $L_{i(m+1)}$ joining the last point of P_i with its first point, making each P_i a closed curve and thereby accounting each end point of the line segments in P_i twice. We can define the *conflation* $C(P_1, P_2) = C(P_2, P_1)$ between P_1 and P_2 by (2), where the transformation τ is an arbitrary combination of translation and rotation around the origin. If $|P_1| = m_1 > m_2 = |P_2|$, then we consider the conflation $C(P_1^k, P_2)$ between P_2 and each m_2-subchain $P_1^k = \langle L_{1k}, L_{1(k+1)}, \ldots, L_{1(k+m_2-1)}\rangle$ of P_1, and take the best (smallest) of them to be $C(P_1, P_2)$.This is applicable when P_2 is a subimage of P_1. An alternative but computationally more expensive approach would be to approximate P_1 by a polyline P_1' with m_2 line segment and then conflate P_1' and P_2. One can also approximate each P_i with a polyline P_1' having $m = (m_1 + m_2)/2$ line segments and then conflate P_1' and P_2'. In any case, the key problem in defining the conflation $C(P_1, P_2)$ rests on having an appropriate distance measure $D(L_1, L_2)$ between two line segments L_1 and L_2. In addition, it must be possible to find an efficient algorithm to compute the conflation-mapping τ, which may not be always unique, using that distance measure.

$$D(P_1, P_2) = \sum_{j=1}^{m} D(L_{1j}, L_{2j}), \tag{1.1}$$

$$D(P_1, P_2) = \sum_{j=1}^{m+1} D(L_{1j}, L_{2j}), \tag{1.2}$$

$$C(P_1, P_2) = \begin{cases} \min_{\tau}\{D(P_1, \tau(P_2))\} & \text{for } |P_1| = |P_2|, \\ \min_{k=1}^{m_1-m_2+1} \{C(P_1^k, P_2)\} & \text{for } |P_1| = m_1 > m_2 = |P_2|. \end{cases} \tag{2}$$

If p_i, $1 \leqslant i \leqslant m+1$, are the successive end points of the line segments in $P = \langle L_1, L_2, \ldots, L_m\rangle$, then we regard each $L_i = \langle p_i, p_{i+1}\rangle$ to be directed from p_i to p_{i+1}. We write $L_i^{(r)}$ for the line segment from p_{i+1} to p_i, having the opposite direction of L_i, and $|L_i|$ = length of L_i (which should not be confused with $|P| = m$).

A distance measure $D(L_1, L_2)$ (also called a *metric* [4]) should satisfy the basic requirements (D.1)–(D.3) below. It follows that both $D(P_1, P_2)$ given by Eqs. (1.1)–(1.2) then satisfy (D.1)–(D.3); the converse is also true (take $m = 1$). For the purpose of conflation, we need the additional properties (D.4)–(D.5). The invariance property (D.4) under the rotation and translation operation τ implies that $D(L_1, L_2)$ depends only on the relative positions of L_1 and L_2. On the other hand, (D.5) is a directional symmetry property. If $D(L_1, L_2)$ satisfies (D.1)–(D.5), then the same is true for $cD(L_1, L_2)$, where $c > 0$ is a constant.

(D.1) $D(L_1, L_2) \geqslant 0$ and it equals 0 if and only if $L_1 = L_2$.
(D.2) $D(L_1, L_2) = D(L_2, L_1)$. (Symmetry)
(D.3) $D(L_1, L_3) \leqslant D(L_1, L_2) + D(L_2, L_3)$. (Triangle inequality)
(D.4) $D(L_1, L_2) = D(\tau(L_1), \tau(L_2))$, where τ is a rotation or translation.
(D.5) $D(L_1, L_2) = D(L_1^{(r)}, L_2^{(r)})$, where $L_i^{(r)}$ is L_i with the opposite direction.

Note that we do not require any particular relationship between $D(L_1, L_2)$ and $D(L_1^{(r)}, L_2)$ in order to let $D(L_1, L_2)$ be sensitive to the relative directions of L_1 and L_2. Indeed, if we insist that $D(L_1, L_2) \leqslant D(L_1^{(r)}, L_2)$, say, then we also have $D(L_1^{(r)}, L_2) \leqslant D(L_1, L_2)$, by replacing L_1 with $L_1^{(r)}$, and this would give $D(L_1, L_2) = D(L_1^{(r)}, L_2)$. This would mean that the relative directions of L_1 and L_2 are not relevant.

2.1. Distance between line segments

We first define a simple distance measure $D_1(L_1, L_2)$ for two line segments $L_1 = \langle p_{11}, p_{12}\rangle$ and $L_2 = \langle p_{21}, p_{22}\rangle$, and then generalise it to $D_2(L_1, L_2)$ to eliminate some of its shortcomings.

The definition of $D_1(L_1, L_2)$ in Eq. (3) is based on the Euclidean-distance function $d(p, p')$ between two points. One can also use the more general Minkowski-distance function $d_q(p, p') = (|x - x'|^q + |y - y'|^q)^{1/q}$, for some constant $q \geqslant 1$, where $p = (x, y)$ and $p' = (x', y')$; note that $d(p, p') = d_2(p, p')$. It is easy to see that $D_1(L_1, L_2)$ satisfies (D.1)–(D.5); in particular, the triangle inequality (D.3) follows directly from the triangle inequality for $d(p, p')$. If $L_1 = \langle p_1, p_2\rangle$ and $L_2 = \langle p_2, p_1\rangle = L_1^{(r)}$, then $D_1(L_1, L_2) = 2d(p_1, p_2)$

$$D_1(L_1, L_2) = d(p_{11}, p_{21}) + d(p_{12}, p_{22}). \tag{3}$$

Example 1. Figs. 1(i)–(iii) show three different situations which give the same $D_1(L_1, L_2)$ since $D_1(L_1, L_2)$ accounts only for the end points of L_1 and L_2. The line segments in Fig. 1(ii) are obtained by moving the right end points p_{12} and p_{22} in Fig. 1(i) horizontally to the right by the same amount (and not by the same factor of their lengths). One may feel that since the line segments in Fig. 1(ii) have larger lengths than those in Fig. 1(i) and they cover a larger area between them than those in Fig. 1(i), we should have a larger distance between them. But as we will show below, this is not a valid argument because distance is a first-order quantity and the area is a second-order quantity. The line segments in Fig. 1(iii) are obtained by moving the point p''_{21} along the circle of radius $\delta_1 = d(p''_{11}, p''_{21})$ and centered at p''_{11}. One

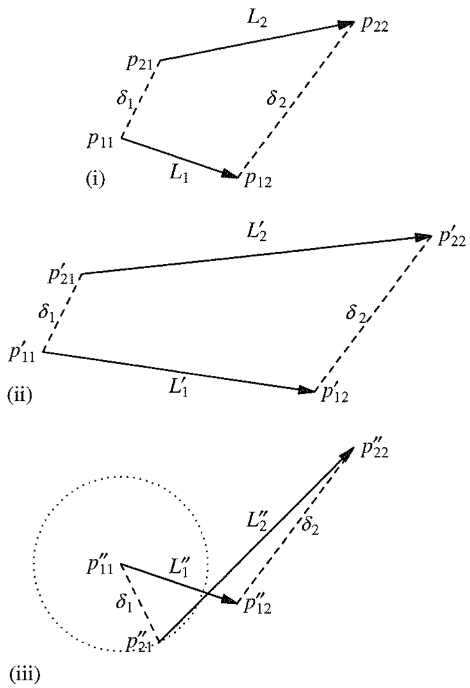

Fig. 1. Three different cases of L_1 and L_2 for a given pair of distances $\delta_1 = d(p_{11}, p_{21})$ and $\delta_2 = d(p_{12}, p_{22})$ between their end points: (i) a pair of non-intersecting line segments L_1 and L_2; (ii) another non-intersecting case with each L_i stretched horizontally to the right; (iii) the case of intersecting line segments; here, p_{21}'' is moved along the cycle of radius δ_1 and centered at p_{11}''.

is more justified in requiring that Fig. 1(iii) give a smaller distance measure than that in Fig. 1(i) since there are many more points along the two line segments that are closer to each other than the case in Fig. 1(i). A similar situation arises if we move the point p_{22} in a circle of radius $\delta_2 = d(p_{12}'', p_{22}'')$ around p_{12}'' and make the line segments cross each other. The distance function $D_2(L_1, L_2)$ to be defined below corrects this problem in $D_1(L_1, L_2)$. Note that if L_1 and L_2 are the horizontal and the vertical line segments in the letter "T", then $D_1(L_1, L_2) = D_1(L_1^{(r)}, L_2)$, but this clearly does not hold in general.

We now argue that there is no need to distinguish between the cases in Figs. 1(i)–(ii). First, if the right end points of L_1 and L_2 are moved horizontally far to the right by the same amount and we look at L_1 and L_2 near their right end points p_{12} and p_{22}, then the line segments would appear almost parallel, with a natural distance between them given by q_2 = the length of the perpendicular from the point p_{12} to L_2. Likewise, by looking at L_1 and L_2 near their left end points p_{11} and p_{21}, the line segments would appear almost parallel, with a distance between them given by q_1 = the length of the perpendicular from the point p_{21} to L_1. This may suggest that the right-hand side of Eq. (3) should be replaced by $q_1 + q_2$. However, since q_2 does not change if we just extend L_2 to the right keeping its direction and leave L_1 unchanged, it follows that q_2 is not a good replacement for the term $d(p_{12}, p_{22})$ in Eq. (3). Likewise, q_1 is not a good replacement for the term $d(p_{11}, p_{21})$ in Eq. (3). This indicates that contrary to the initial intuition it is not necessary to distinguish between the two cases Figs. 1(i)–(ii).

2.2. A generalization

We now introduce a generalization $D_2(L_1, L_2)$ of $D_1(L_1, L_2)$ which can distinguish the cases in Figs. 1(i) and (iii). Consider each L_i as a curve $L_i(t) = (x_i(t), y_i(t))$, $0 \leqslant t \leqslant 1$ given below, where $p_{ij} = (x_{ij}, y_{ij})$, $1 \leqslant i, j \leqslant 2$, $p_{i1} = (x_i(0), y_i(0))$, $p_{i2} = (x_i(1), y_i(1))$,

$$x_1(t) = x_{11} + (x_{12} - x_{11})t \quad \text{and} \quad y_1(t) = y_{11} + (y_{12} - y_{11})t,$$

$$x_2(t) = x_{21} + (x_{22} - x_{21})t \quad \text{and} \quad y_2(t) = y_{21} + (y_{22} - y_{21})t.$$

We take the sum of the distances between the corresponding points in $L_1(t)$ and $L_2(t)$ for $t = t_j = j/n$, $0 \leqslant j \leqslant n$ for a fixed $n \geqslant 1$, to define

$$D_2(L_1, L_2) = \sum_{j=0}^{n} \sqrt{[x_2(t_j) - x_1(t_j)]^2 + [y_2(t_j) - y_1(t_j)]^2}. \tag{4}$$

For $n = 1$, we have $D_2(L_1, L_2) = D_1(L_1, L_2)$. On the other hand, if $p_{11} = p_{21}$, then $D_2(L_1, L_2) = c_n D_1(L_1, L_2)$, where $c_n = 1 + 1/2 + 1/3 + \cdots + 1/n$. Note that although $c_n \to \infty$ as n increases, this is not a problem because we use the same n for each line segment pair $\{L_{1j}, L_{2j}\}$ in measuring the distance between two polylines P_1 and P_2.

Theorem 1. *Suppose the line segment pairs* $\{L_1, L_2\}$ *and* $\{L_1'', L_2''\}$ *have the same distances for their end points, i.e.,* $d(p_{11}, p_{21}) = d(p_{11}'', p_{21}'')$ *and* $d(p_{12}, p_{22}) = d(p_{12}'', p_{22}'')$ *as in Figs.* 1(i) *and* (iii), *where* $L_1 \cap L_2 = \emptyset$ *and* $L_1'' \cap L_2'' \neq \emptyset$. *Then,* $D_2(L_1'', L_2'') < D_2(L_1, L_2)$ *for* $n \geqslant 2$.

Proof. For each $t_j \neq 0$ and 1, the points $L_1(t_j) = (x_1(t_j), y_1(t_j))$ and $L_2(t_j) = (x_2(t_j), y_2(t_j))$ contribute a larger value to $D_2(L_1, L_2)$ than the contribution of the points $L_1''(t_j) = (x_1''(t_j), y_1''(t_j))$ and $L_2''(t_j) = (x_2''(t_j), y_2''(t_j))$ to $D_2(L_1'', L_2'')$. The theorem follows immediately. □

Theorem 2. $D_1(L_1, L_2) \leqslant D_2(L_1, L_2) \leqslant (1 + 1/2 + \cdots + 1/n) D_1(L_1, L_2)$.

Proof. The inequality $D_1(L_1, L_2) \leqslant D_2(L_1, L_2)$ is immediate. To prove the other inequality, first consider the case

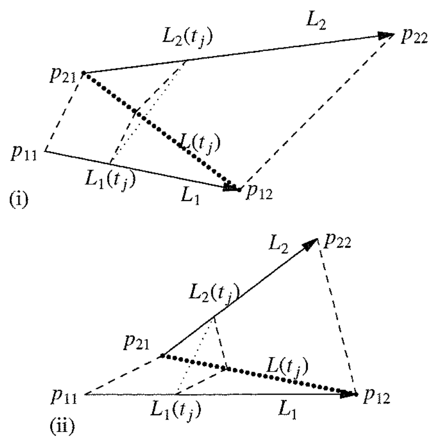

Fig. 2. Illustration of the proof of Theorem 2 when $L_1 \cap L_2 = \emptyset$: (i) the case where L_1 and L_2 intersect, when extended, at a point not in L_1 or L_2; (ii) the case where L_1 and L_2 intersect, when extended, at a point in L_1.

where $L_1 \cap L_2 = \emptyset$, as in Fig. 1(i). Figs. 2(i)–(ii) show the case where L_1 and L_2 intersect if they are extended to the left; let $L = \langle p_{21}, p_{12}\rangle$, indicated by the bold dotted line. The contribution to $D_2(L_1, L_2)$ for $t_j = j/n$, $0 \leqslant j \leqslant n$, is given by

$$\begin{aligned} d(L_1(t_j), L_2(t_j)) &\leqslant d(L_1(t_j), L(t_j)) + d(L(t_j), L_2(t_j)) \\ &= [1 - t_j]d(p_{11}, p_{21}) + t_j d(p_{12}, p_{22}). \end{aligned}$$

The theorem follows in this case since the sum of the right-hand side above for $0 \leqslant j \leqslant n$ gives $[1 + 1/2 + \cdots + 1/n][d(p_{11}, p_{21}) + d(p_{12}, p_{22})] = [1 + 1/2 + \cdots + 1/n]D_1(L_1, L_2)$. If L_1 and L_2 are parallel or they intersect when extended to the right, the same argument holds. Finally, if $L_1 \cap L_2 \neq \emptyset$ as in Fig. 1(iii), we get the result by combining the above case with Theorem 1 and the fact that $D_1(L_1, L_2)$ is the same for the two cases in Fig. 1(i) and (iii). □

Several remarks are due at this point. First, if we vary the parameter n in the definition of $D_2(L_1, L_2)$ and make n, say, proportional to $|L_1|+|L_2|$ in order to make $D_2(L_1, L_2)$ sensitive to the lengths $|L_1|$ and $|L_2|$, this can lead to the failure of the triangle inequality (D.3). This happens, for example, if $|L_2|$ is very small compared to $|L_1| = |L_3|$. Second, the larger the value of n, more significant is the distinction between the $D_2(L_1, L_2)$-measures for the cases in Figs. 1(i) and (iii). Finally, although the inequalities in Theorem 2 imply that the distance measures $D_1(L_1, L_2)$ and $D_2(L_1, L_2)$ are topologically equivalent [4], the ability of $D_2(L_1, L_2)$ to distinguish between the cases in Figs. 1(i) and (iii) makes it more suitable for conflation. It should be noted that $D_2(L_1, L_2)$ does not distinguish between the cases in Figs. 1(i) and (ii).

3. Inadequacy of Hausdorff's measure

We now show that Hausdorff's distance measure, which has been suggested in the literature (http://www.vividsolutions.com), is not suitable for conflation. First, it is not sufficiently sensitive to the relative positions of L_1 and L_2. Hausdorff's measure, which was originally defined to measure distance between two arbitrary subsets (in a metric space), does not account for the geometric properties of the subsets. In particular, it does not account for the geometric feature of line segments when applied to L_1 and L_2. Second, it does not give a computationally efficient method to determine the transformation τ to conflate two polylines.

Given a line segment L and a point p in the plane, a simple definition of a point-to-set distance is $d_{pts}(p, L) = \min\{d(p, q) : q \in L\}$, which is positive unless $p \in L$. It is easy to see that $d_{pts}(p, L)$ equals the perpendicular distance of p from L, if the perpendicular meets the line segment L, and otherwise $d_{pts}(p, L)$ equals the minimum distance between p and the end points of L (see Figs. 3(i)–(ii)). Hausdorff's distance $D_H(L_1, L_2)$ between two line segments is defined by (5), where $d_H(L_1, L_2) = \max\{d_{pts}(p, L_2) : p \in L_1\} = \max\{d_{pts}(p, L_2) : p = p_{11} \text{ or } p_{12}\}$, giving a simple method for computing $d_H(L_1, L_2)$. In particular, $d_H(L_1, L_2)$ may not be the same as $d_H(L_2, L_1)$.

$$D_H(L_1, L_2) = \max\{d_H(L_1, L_2), d_H(L_2, L_1)\}. \quad (5)$$

It is not hard to see that $D_H(L_1, L_2)$ satisfies all the properties (D.1)–(D.5). However, the measure $D_H(L_1, L_2)$ is insensitive in two ways to the geometric properties of L_1 and L_2. First, if we reverse the direction of L_2, say, then $D_H(L_1, L_2)$ remains unchanged. Second, as seen in Fig. 4, $D_H(L_1, L_2) = d(p_{11}, p_{21})$, remains unchanged if the end point p_{22} of L_2 lies anywhere between the points A and B of the upper part of the circular arc of radius $D_H(L_1, L_2)$ at p_{12} intersecting the extension of L_2 or, more generally, in the region of that circle above the line L_2. (In contrast, $D_1(L_1, L_2)$ remains the same only for p_{22} at the end points A and B.)

In order to show that $D_H(L_1, L_2) \leqslant D_1(L_1, L_2)$, let $p = p_{21}$ and $L = L_1$ in Fig. 3. It follows that $d_{pts}(p_{21}, L_1) \leqslant d(p_{21}, p_{11})$ and likewise we have $d_{pts}(p_{22}, L_1) \leqslant d(p_{22}, p_{12})$ which gives $d_H(L_2, L_1) \leqslant D_1(L_1, L_2)$. Similarly, we get $d_H(L_1, L_2) \leqslant D_1(L_1, L_2)$, and hence $D_H(L_1, L_2) \leqslant D_1(L_1, L_2)$. However, the ratio $D_H(L_1, L_2)/D_1(L_1, L_2)$ is not bounded below by a positive number. To see this, consider the case where $p_{11} = p_{22}$ and $|L_1| = |L_2| = r$. If $\theta =$ the angle between L_1 and L_2 and $0 < \theta < \pi/2$, then $D_1(L_1, L_2) = 2r$, whereas $D_H(L_1, L_2) = r\sin(\theta)$ and hence the ratio $D_H(L_1, L_2)/D_1(L_1, L_2)$ can be arbitrarily small. Although, there is no easy way of finding the best transformation τ to conflate two polylines using Hausdorff's distance, the best conflation of two line segments L_1 when L_2 using Hausdorff-distance places L_1 symmetrically on top of L_2 (along the same line). The same is true if we use the distance measure $D_2(L_1, L_2)$ for $n \geqslant 2$, except that now

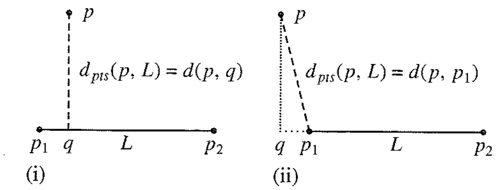

Fig. 3. Illustration of $d_{pts}(p, L)$: (i) the perpendicular from p to $L = \langle p_1, P_2 \rangle$ intersects L at q; (ii) the perpendicular from p to $L = \langle p_1, P_2 \rangle$ does not intersect L.

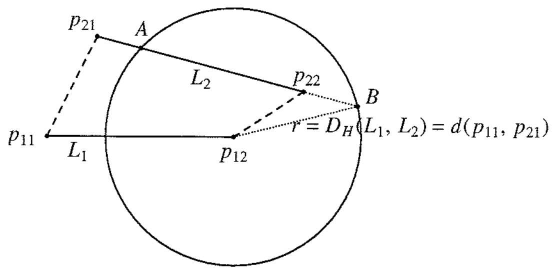

Fig. 4. $D_H(L_1, L_2)$ remains unchanged for any position of p_{22} on the chord AB.

L_1 and L_2 must be in the same direction. For $n = 1$, i.e., if we use $D_1(L_1, L_2)$, then τ is not unique and we only need to make the shorter of L_1 and L_2 completely overlap the other and keep them in the same direction.

4. Computing optimal τ

Since minimizing $D_2(P_1, \tau(P_2))$ is closely related to minimizing $D_1(P_1, \tau(P_2))$, with the only difference being the additional partition points in the former, we first focus on minimizing $D_1(P_1, \tau(P_2))$. If we know $\tau(P_2)$, then we can express τ as a combination of a translation $\tau_{x,y}$, which moves each point (x', y') to $(x + x', y + y')$, followed by a rotation τ_θ around the new start point of $\tau_{x,y}(P_2)$. Once $\tau_{x,y}$ and τ_θ are determined, it is a simple matter to express τ in terms of a translation and a rotation around the origin (0, 0). The translation $\tau_{x,y}$ is easily determined from the start points of P_2 and $\tau(P_2)$, and the rotation-angle θ is determined from the slope of the first line segment $L_{21} \in P_2$ and its slope in $\tau(P_2)$. Throughout this section, we use (1.2) for the distance between two polylines.

4.1. Best translation $\tau_{x,y}$

Let $v_j = \overline{p_{1j}p_{2j}}$, the vector from the jth point $p_{1j} \in P_1$ to the jth point $p_{2j} \in P_2$. If we write $p_{ij} = (x(p_{ij}), y(p_{ij}))$, $1 \leqslant i \leqslant 2$ and $1 \leqslant j \leqslant m+1$, then $v_j = (x_j y_j)$, where $x_j = x(p_{2j}) - x(p_{1j})$ and $y_j = y(p_{2j}) - y(p_{1j})$. Moreover, $v = -(x, y)$ corresponding to $\tau_{x,y}$ is given by the point which minimizes the sum of distances $d_1 + d_2 + \cdots + d_m + d_{m+1}$, where $d_j = d(v, v_j) = ||v_j - v|| = \sqrt{(x_j + x)^2 + (y_j + y)^2}$.

Since an analytical solution for the optimal v is difficult, we employ a slight variation of D_1-measure to bypass this problem; the basic idea of this variation came from the fuzzy c-means method [5]. Let

$$D_1^{sq}(P_1, P_2) = \sqrt{2\sum_{j=1}^{m+1} d^2(p_{1j}, p_{2j})} = \sqrt{2\sum_{j=1}^{m+1} ||v_j||^2} = \sqrt{\sum_{j=1}^{m+1} [D_1^{sq}(L_{1j}, L_{2j})]^2}, \tag{6}$$

where $D_1^{sq}(L_1, L_2) = \sqrt{d^2(p_{11}, p_{21}) + d^2(p_{12}, p_{22})}$. It is not hard to see that $D_1^{sq}(L_1, L_2)$ is a metric (see Appendix) and that it also satisfies (D.4)–(D.5). Likewise, $D_1^{sq}(P_1, P_2)$ satisfies (D.1)–(D.5). Since minimizing $D_1^{sq}(P_1, \tau_{x,y}(P_2))$ amounts to minimizing $\sum ||v_j - v||^2$, the minimum is obtained when v equals the centroid of the points v_j, i.e., $x = (-\sum x_j)/(m+1)$ and $y = (-\sum y_j)/(m+1)$.

We can likewise define $D_2^{sq}(L_1, L_2)$ by generalizing $D_1^{sq}(L_1, L_2)$ using the $(n-1)$ equally spaced intermediate points in each of L_1 and L_2 as in Eq. (4). To be precise, we have

$$D_2^{sq}(L_1, L_2) = \sqrt{\sum_{j=0}^{n} [[x_2(t_j) - x_1(t_j)]^2 + [y_2(t_j) - y_1(t_j)]^2]}$$
$$\text{where } t_j = j/n. \tag{7}$$

To get the corresponding measure for polylines, again using form (1.2), let $p_{1j}^{(k)}$ denote the kth partition point of the line segment $L_{1j} \in P_1$, with $p_{1j}^{(0)}$ = the start point of L_{1j} and $p_{1j}^{(n)}$ = the end point of L_{1j} = the start point of $L_{1(j+1)} = p_{1(j+1)}^{(0)}$, and similarly let $p_{2j}^{(k)}$ be the points arising from P_2. Then, $x_j^{(k)} = x(P_{2j}^{(k)}) - x(p_{1j}^{(k)})$ and $y_j^{(k)} = y(p_{2j}^{(k)}) - x(p_{1j}^{(k)})$ are given by

$$x_j^{(k)} = [x(p_{2j}) - x(p_{1j})] + [[x(p_{2,(j+1)}) - x(p_{2j})] - [x(p_{1,(j+1)}) - x(p_{1j})]]k/n, \quad 0 \leqslant k \leqslant n,$$
$$y_j^{(k)} = [y(p_{2j}) - y(p_{1j})] + [[y(p_{2,(j+1)}) - y(p_{2j})] - [y(p_{1,(j+1)}) - y(p_{1j})]]k/n, \quad 0 \leqslant k \leqslant n.$$

Finally, let $v_j^{(k)} = (x_j^{(k)}, y_j^{(k)})$ and we have $D_2^{sq}(P_1, P_2)$ is given by Eq. (8). If we want to avoid duplicate account of the start and end points of the line segments L_{1j} and L_{2j} in Eq. (8) compared to each intermediate partition point being counted only once, then the sum for k should be only for $0 \leqslant k < n$. In either case, $D_2^{sq}(P_1, P_2)$ satisfies (D.1)–(D.5) and $D_2^{sq}(L_1, L_2)$ distinguishes between the cases in Figs. 1(i) and (iii):

$$D_2^{sq}(P_1, P_2) = \sqrt{\sum_{j=1}^{m+1} \sum_{k=0}^{n} ||v_j^{(k)}||^2} = \sqrt{\sum_{j=1}^{m+1} [D_2^{sq}(L_{1j}, L_{2j})]^2}. \quad (8)$$

The optimal translation $\tau_{x,y}$ of P_2 which minimizes $D_2^{sq}(P_1, \tau_{x,y}(P_2))$ is related to the centroid of the points $(x_j^{(k)}, y_j^{(k)})$, $1 \leqslant j \leqslant m+1, 0 \leqslant k \leqslant n$, as before and is given by Eq. (9), where $x_j = x_j^{(0)}$ and $y_j = y_j^{(0)}$. If we use the sum for $0 \leqslant k < n$ in Eq. (8), then interestingly the final result in Eq. (9) remains the same:

$$x = \frac{-1}{(m+1)(n+1)} \sum_{j=1}^{m+1} \sum_{k=0}^{n} x_j^{(k)} = \frac{-1}{m+1} \sum_{j=1}^{m+1} \left[x_j + \frac{1}{2}(x_{j+1} - x_j) \right] = \frac{-1}{m+1} \sum_{j=1}^{m+1} x_j$$

and

$$y = \frac{-1}{(m+1)(n+1)} \sum_{j=1}^{m+1} \sum_{k=0}^{n} y_j^{(k)} = \frac{-1}{m+1} \sum_{j=1}^{m+1} \left[y_j + \frac{1}{2}(y_{j+1} - y_j) \right] = \frac{-1}{m+1} \sum_{j=1}^{m+1} y_j. \quad (9)$$

4.2. Best rotation τ_θ

As in the previous section, we first consider the minimization of $D_1^{sq}(P_1, \tau_\theta(P_2))$. Since the rotation of P_2 around its start point p_{21} does not change the distance $d_1 = d(p_{11}, p_{21})$, we are now concerned only with minimizing the sum $d_2^2 + d_3^2 + \cdots + d_{m+1}^2$. For $2 \leqslant j \leqslant m+1$, let $\theta_j + \theta$ be the angle from the line $\overline{p_{21}p_{1j}}$, joining p_{21} to the jth point $p_{1j} \in P_1$, and the line $\overline{p_{21}p_{2j}}$, joining p_{21} to the jth point $p_{2j} \in \tau_\theta(P_2)$ (see Fig. 5(i)). We also write $d_{1j} = d(p_{21}, p_{1j})$ and $d_{2j} = d(p_{21}, p_{2j})$. Note that $\theta_1 + \theta$ is not defined; likewise, $\theta_j + \theta$ is not defined if $d_{1j} = 0$, and in that case the corresponding term in the sum below is taken to be zero.

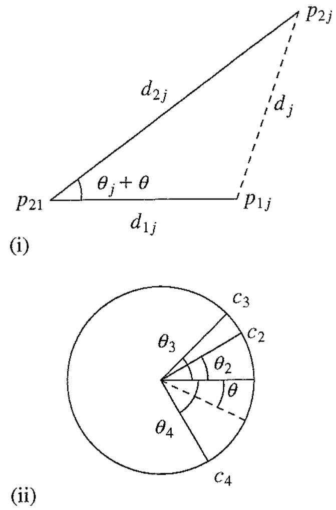

Fig. 5. Computation of the best τ_θ: (i) the relationship of d_{1j}, d_{2j}, d_j, and the angle $(\theta_j + \theta)$ after rotating P_2 by θ; (ii) a geometric view associated with the minimization of $\sum c_j \cos(\theta_j + \theta)$ for $m = 3$.

From Fig. 5(i), we get

$$\sum_{j=2}^{m+1} d_j^2 = \sum [d_{1j}^2 + d_{2j}^2 - 2d_{1j}d_{2j} \cos(\theta_j + \theta)] = \sum [d_{1j}^2 + d_{2j}^2] - \sum 2d_{1j}d_{2j} \cos(\theta_j + \theta) = c - 2\sum_{j=2}^{m+1} c_j \cos(\theta_j + \theta)$$

where c and c_j are constants.

Thus, minimizing $D_1^{sq}(P_1, \tau_\theta(P_2))$ is the same as maximizing the sum $\sum c_j \cos(\theta_j + \theta)$ (for $2 \leqslant j \leqslant m+1$), which is simply a weighted sum of the projections (see Fig. 5(ii)) of the given radial lines of the unit circle with the angles θ_j on the dashed radial line with the angle $-\theta$. However, since the sum of projections equals the projection of the sum of vectors $c_j(\cos(\theta_j), \sin(\theta_j))$ on the dashed line, the maximum occurs when the direction of the dashed line is the same as that of the sum of vectors, i.e., the angle θ is given by

$$\theta = -\text{direction of the vector} \left[\sum_{j=2}^{m+1} c_j(\cos(\theta_j), \sin(\theta_j)) \right].$$

To minimize $D_2^{sq}(P_1, \tau_\theta(P_2))$, the best rotation-angle θ is then given by Eq. (10). Once again, if we use the sum $0 \leqslant k < n$ in Eq. (9), then the same would be the case in (10):

$$\theta = -\text{direction of the vector} \sum_{j=2}^{m+1} \sum_{k=0}^{n} c_j^{(k)}(\cos(\theta_j^{(k)}), \sin(\theta_j^{(k)})), \quad (10)$$

where

$$c_j^{(k)} = d_{1j}^{(k)} d_{2j}^{(k)}, \quad d_{1j}^{(k)} = d(p_{21}, p_{1j}^{(k)}),$$
$$d_{2j}^{(k)} = d(p_{21}, p_{1j}^{(k)})$$

and

$$\theta_j^{(k)} = \text{angle of the line } \overline{p_{21} p_{2j}^{(k)}} \text{ from the line } \overline{p_{21} p_{1j}^{(k)}}.$$

4.3. Algorithm CONFLATE

We now present the algorithm CONFLATE for determining the final position $\tau(P_2)$ of P_2 which minimizes the distance $D_2^{sq}(P_1, \tau(P_2))$. We have included steps (3)–(5) in CONFLATE to specifically avoid a local optimum position of $\tau(P_2)$ after step (1). Example 2 shows a few known cases of this local optimum phenomenon. Since there may be other cases that are not resolved by steps (3)–(5) alone, one can in general apply a random translation $\tau_{x,y}$ and a random rotation τ_θ to the current position of P_2 after an application of CONFLATE and then reapply CONFLATE to see if this gives *a* smaller distance $D_2^{sq}(P_1, \tau(P_2))$. This procedure may be repeated a few times to provide more confidence that the global optimum is reached.

Algorithm CONFLATE.

Input: A pair of polylines P_1 and P_2, each P_i having m line segments L_{ij}, $1 \leqslant j \leqslant m$, and an error threshold $\varepsilon > 0$ for the optimal conflation τ.

Output: A transformed position $\tau(P_2)$ that minimizes $D_2^{sq}(P_1, \tau(P_2))$ within the bound ε of the optimal, where τ consists of a translation and a rotation.

1. Repeat the steps (a)–(b);
   (a) Find the translation $\tau = \tau_{x,y}$, where (x, y) is given by Eq. (9), so that $D_2^{sq}(P_1, \tau(P_2))$ is minimized among all translations. Let $\varepsilon_1 = D_2^{sq}(P_1, P_2) - D_2^{sq}(P_1, \tau(P_2)) \geqslant 0$ and $P_2 = \tau(P_2)$.
   (b) Find the rotation $\tau = \tau_\theta$, where θ is given by Eq. (10), so that $D_2^{sq}(P_1, \tau(P_2))$ is minimized among all rotations. Let $\varepsilon_2 = D_2^{sq}(P_1, P_2) - D_2^{sq}(P_1, \tau(P_2)) \geqslant 0$ and $P_2 = \tau(P_2)$.
   While at least one of ε_1 and $\varepsilon_2 \geqslant \varepsilon$.
2. Let Q be the most recent position of P_2.
3. If $\max(\varepsilon_1, \varepsilon_2) = 0$, then stop; otherwise, give an initial rotation of π to Q around p_{21}, i.e., let $P_2 = \tau_\pi(Q)$, go back to step (1), and let Q' be the resulting best position of P_2 in step (2).
4. If $D_2^{sq}(P_1, Q) < D_2^{sq}(P_1, Q')$, then let $P_2 = Q$ else let $P_2 = Q'$.
5. Repeat steps (1)–(4) as long as the new position of P_2 achieves a decrease in $D_2^{sq}(P_1, P_2)$ by ε or more.

Example 2. Consider the simplest case with $m = 1 = n$, $P_1 = L_1$ and $P_2 = L_2 = L_1^{(r)}$. Step (1) has only one iteration. In step 1(a), we obtain $(x, y) = (0, 0)$ for the optimal translation $\tau_{x,y}$ and in step 1(b) we obtain $\theta = 0$ for the optimal rotation τ_θ, giving $\varepsilon_1 = \varepsilon_2 = 0$. Then, after we force a rotation by $\theta = \pi$ to P_2 around $p_{21} = p_{12}$ in step (3) and we go back to step (1), we again get only one iteration. In step 1(a), we get $(x, y) = (x(p_{21}) - x(p_{11}), y(p_{21}) - y(P_{11}))$ for the optimal translation, which shifts L_2 completely on the top of L_1 matching the direction of L_1, i.e., $\tau_{x,y}(L_2) = L_1$ and giving $D_2^{sq}(L_1, \tau_{x,y}(L_2)) = 0$. In step 1(b), we get $\theta = 0$, and the algorithm now stops in step (3) by finding the optimum position of P_2. Note that for $n = 1$, the initial rotation by $\theta = \pi$ step (3) does not change $D_2^{sq}(P_1, P_2)$; however, for $n > 1$, it actually increases $D_2^{sq}(P_1, P_2)$, which is then reduced to 0 by the next optimal translation in step 1(a).

A similar situation arises if $m = 3$, $n = 1$, P_1 has the shape of the letter "*W*" going from left to right, and P_2 has the shape of an upside-down "*W*" (or equivalently, the shape of the letter "*M*") of the same size but going from right to left. In this case, the optimal translation $\tau_{x,y}$ in step 1(a) positions P_2 on the top of P_1 with partial vertical overlapping but the optimal τ_θ does not do any change $(\theta = 0)$. After we force a rotation of $\theta = \pi$ in step (3), which increases D_2^{sq}-distance, and we go back to step (1) we again get only one iteration. In step 1(a), the optimal translation shifts P_2 completely on top of P_1 matching the direction of P_1, i.e., $\tau_{x,y}(P_2) = P_1$ and giving D_2^{sq}-distance zero. In step 1(b), we get $\theta = 0$ and the algorithm now stops in step (3) by finding the optimum position of P_2.

Example 3. Fig. 6 illustrates the algorithm CONFLATE when applied to a pair of L-shaped polylines. Here, we have used $n = 3$ and $\varepsilon = 0.1$ to keep the number of iterations small. The initial positions of P_1 and P_2 are shown in Fig. 6(i). The step (1) now involves three iterations of steps 1(a) and (b), combining a translation and a rotation in each iteration. The results of the first application of steps 1(a) and 1(b) are shown in Fig. 6(ii), and the final result of step (1) after the three iterations are shown in Fig. 6(iii). Note that the position of P_1 remains fixed throughout. Fig. 6(iv) shows the positions of P_1 and P_2 at the start of the second phase after the forced rotation of P_2 around its start point by π. There are nine iterations of steps 1(a) and (b) now. Fig. 6(v) shows the results after the first iteration of step 1(a) and 1(b) and Fig. 6(vi) shows the final positions at the end of step (3). This also corresponds to the minimum D_2-distance and the final conflation between the initial P_1 and P_2.

4.4. Computational complexity

It is clear that computing the best translation $\tau_{x,y}$ of P_2 by using (9) takes $O(mn)$ time, where $m = |P_1| = |P_2| = \#$(line segments in P_1) = #(line segments in P_2) and n = #(equal length partitions for each segment in P_1) = #(equal length partitions for each segment in P_2). Likewise, it takes $O(mn)$ to compute the best rotation τ_θ of P_2 around the start point of P_2.

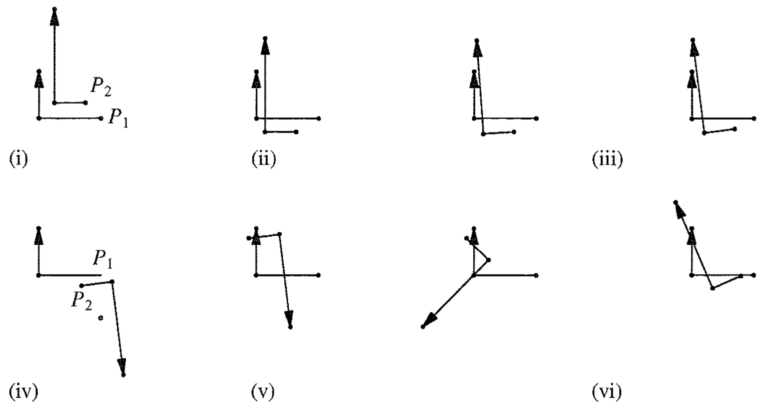

Fig. 6. Illustration of algorithm CONFLATE: (i) initial positions of polylines P_1 and P_2; (ii) results of first translation and first rotation of P_2 from (i); (iii) final positions of P_1 and P_2 after step (1); (iv) positions of P_1 and P_2 after rotation by π in step in (3); (v) results of first translation and first rotation of P_2 from (iv); (vi) final positions of P_1 and P_2 after step (3).

4.5. *Conflation vs. distance*

We briefly point out that if P_1, P_2, and P_3 are three polylines with the same number of line segments, i.e., $|P_1| = |P_2| = |P_3|$, then we have the triangle inequality $C(P_1, P_3) \leqslant C(P_1, P_2) + C(P_2, P_3)$ for the conflation measure given by Eq. (2). The triangle inequality also holds for Eq. (2) when $|P_1| \leqslant |P_2| \leqslant |P_3|$, but it is not true in general. It is for this reason the conflation measure $C(P_1, P_2)$ cannot be taken as a distance when $|P_1| \neq |P_2|$.

5. Some unsuccessful distance functions

One might wonder if there are other distance functions which satisfy (D.1)–(D.5) and has properties like $D_2(L_1, L_2)$ in terms of distinguishing between the cases in Figs. 1(i) and (iii). We show that many other definitions for $D(L_1, L_2)$ which appear attractive at first sight fail to satisfy one or more of the properties (D.1)–(D.5). This provides additional evidence about the goodness of $D_2(L_1, L_2)$.

5.1. *Area between L_1 and L_2*

One may consider the area enclosed between the line segments L_1 and L_2 as a possible distance measure. Figs. 6(i)–(ii) illustrate such a definition of distance $D_3(L_1, L_2)$. However, $D_3(L_1, L_2)$ violates (D.1); it also violates the triangle inequality (D.3), as shown in Fig. 7(iii), which is not surprising since distance is of first-order of dimensionality and area is of second-order of dimensionality. The measure $D_3(L_1, L_2)$ satisfies the other three properties (D.2) and (D.4)–(D.5); it nevertheless distinguishes the cases in Figs. 1(i)–(iii).

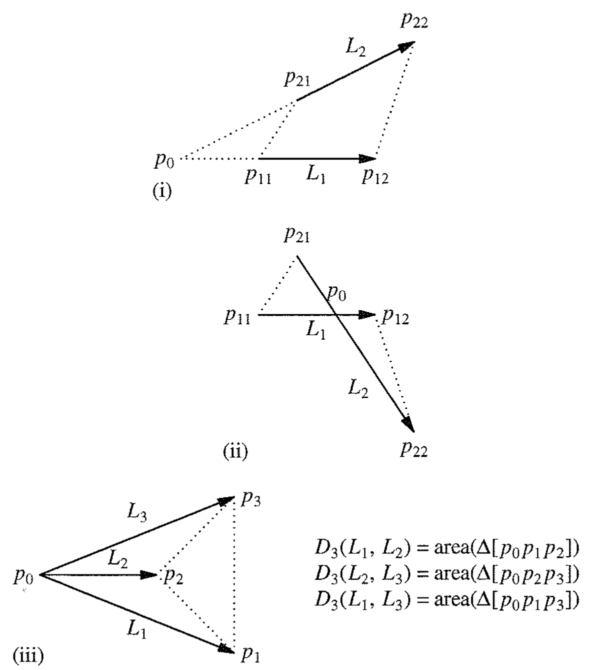

Fig. 7. The measure $D_3(L_1, L_2)$= "area between the line segments L_1 and L_2" does not satisfy the triangle inequality: (i) $D_3(L_1, L_2) = \text{area}(\Delta[p_0 p_{12} p_{22}]) - \text{area}(\Delta[p_0 p_{11} p_{21}])$; (ii) $D_3(L_1, L_2) = \text{area}(\Delta[p_0 p_{11} p_{21}]) + \text{area}(\Delta[p_0 p_{12} p_{22}])$; (iii) $D_3(L_1, L_3) \nleqslant D_3(L_1, L_2) + D_3(L_2, L_3)$.

5.2. *An alternative area-based measure*

Now, consider the sum of the area $\square(x_1, x_2)$ covered between the parametrized linear curves $x_1(t)$ and $x_2(t)$ used in Section 2.2 and the area $\square(y_1, y_2)$ covered between the parametrized linear curves $y_1(t)$ and $y_2(t)$. Fig. 8 shows the curves $x_1(t)$, $x_2(t)$, $y_1(t)$, and $y_2(t)$ for the line segments L_1 and L_2 in Fig. 1(i). We refer to these curves simply as x_1, x_2, y_1, and y_2 below, when no confusion is likely. Note that each of these curves is a straight line. The resulting distance measure $D_4(L_1, L_2)$ interestingly satisfies the triangle inequality. The only property that it fails to

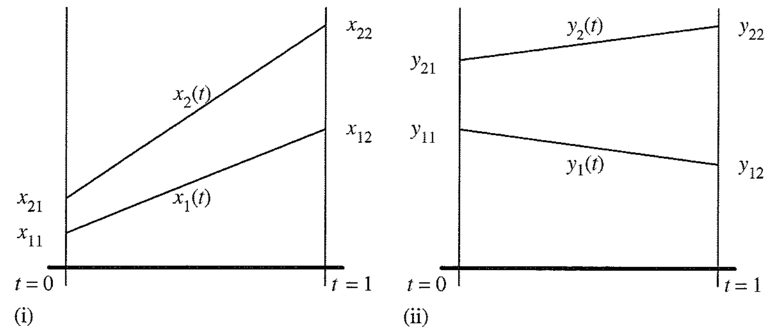

Fig. 8. An alternative area-based approach to defining a distance measure using the curves $x_i(t)$ and $y_i(t)$, $i = 1, 2$: (i) the parametrized linear curves $x_1(t)$ and $x_2(t)$ for the lines in Fig. 1(i); (ii) the parametrized linear curves $y_1(t)$ and $y_2(t)$ for the lines in Fig. 1(i).

satisfy is (D.4):

$$D_4(L_1, L_2) = \square(x_1, x_2) + \square(y_1, y_2) = \int_0^1 |x_1(t) - x_2(t)|\mathrm{d}t + \int_0^1 |y_1(t) - y_2(t)|\mathrm{d}t \qquad (11.1)$$

In contrast to the lines $\{L_1, L_2, L_3\}$ in Fig. 7(iii), which gave rise to the violation of the triangle inequality, the lines $x_i(t)$ and $y_i(t)$ in Figs. 8(i)–(ii) have their right end points on a vertical line (at $t = 1$) and similarly for their left end points (at $t = 0$). The measure $D_4(L_1, L_2)$ is a special case of the more general distance measure, for $q \geqslant 1$, given by

$$D_4^{(q)}(L_1, L_2) = \left(\int_0^1 |x_1(t) - x_2(t)|^q \,\mathrm{d}t\right)^{1/q} + \left(\int_0^1 |y_1(t) - y_2(t)|^q \,\mathrm{d}t\right)^{1/q}. \qquad (11.2)$$

The case $q = 1$ is computationally the simplest. For example, if $x_{11} \leqslant x_{21}$ and $x_{12} \leqslant x_{22}$ (or, $x_{11} \geqslant x_{21}$ and $x_{12} \geqslant x_{22}$), then $\square(x_1, x_2) = |(x_{21} + x_{22})/2 - (x_{11} + x_{12})/2|$. The computation is slightly more complicated if two inequalities are in the reverse direction, i.e., the curves $x_1(t)$ and $x_2(t)$ cross each other. Note that both $D_4(L_1, L_2)$ and $D_4^{(q)}(L_1, L_2)$ have dimensionality one unlike $D_3(L_1, L_2)$. The distance measure $D_4(L_1, L_2)$ can distinguish between the cases in Figs. 1(i) and (iii), but cannot distinguish between the cases in Figs. 1(i)–(ii) when the line $x_1(t)$ does not cross $x_2(t)$ and line $y_1(t)$ does not cross $y_2(t)$.

Fig. 9 shows that $D_4(L_1, L_2)$ does not satisfy the property (D.4) when $\tau = \tau_\theta$ is a rotation. Here, $D_4(L_1, L_2) = [\cos(\theta) - \cos(\theta + \phi)]/2 + [\sin(\theta + \phi) - \sin(\theta)]/2$, which is not independent of θ. The measure $D_4(L_1, L_2)$ clearly satisfies (D.4) when $\tau = \tau_{x,y}$ is a translation.

5.3. Another variation

If we use the curves $x_i(t)$ and $y_i(t)$ to define a distance in a fashion similar to $D_1(L_1, L_2)$, then we do not alleviate the

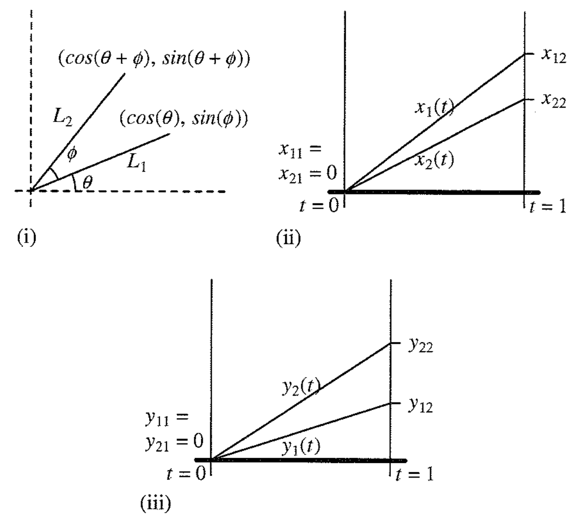

Fig. 9. Illustration of $D_4(L_1, L_2)$ failing to satisfy the property (D.4): (i) two line segments of unit length with $p_{11} = p_{21}$; (ii) the lines $x_1(t)$ and $x_2(t)$ for L_1 and L_2 in (i); (iii) the lines $y_1(t)$ and $y_2(t)$ for L_1 and L_2 in (i).

problem of not distinguishing between the cases in Figs. 1(i) and (iii). This is because, first, we get the distance between $x_1(t)$ and $x_2(t)$ given by (12.1) and that between $y_1(t)$ and $y_2(t)$ given by Eq. (12.2). Finally, $D_5(L_1, L_2)$ is given by Eq. (12.3). Note that $D_5(L_1, L_2) = 0$ if and only if $L_1 = L_2$; the triangle inequality for $D_5(L_1, L_2)$ follows directly from that of D_1 in Eqs. (12.1)–(12.2).

$$D_1(x_1, x_2) = |x_1(0) - x_2(0)| + |x_1(1) - x_2(1)|, \qquad (12.1)$$

$$D_1(y_1, y_2) = |y_1(0) - y_2(0)| + |y_1(1) - y_2(1)|, \qquad (12.2)$$

$$D_5(L_1, L_2) = D_1(x_1, x_2) + D_1(y_1, y_2). \qquad (12.3)$$

It is worth pointing out that since $(a + b)/\sqrt{2} \leqslant \sqrt{a^2 + b^2} \leqslant a + b$ for all $a, b \geqslant 0$ and $d(p_{11}, p_{21}) = \sqrt{[x_1(0) - x_2(0)]^2 + [y_1(0) - y_2(0)]^2}$ and $d(p_{12}, p_{22}) = \sqrt{[x_1(1) - x_2(1)^2] + [y_1(1) - y_2(1)]^2}$, it follows that $D_5(L_1, L_2)/\sqrt{2} \leqslant D_1(L_1, L_2) \leqslant D_5(L_1, L_2)$. Hence, $D_1(L_1, L_2)$ and $D_5(L_1, L_2)$ are equivalent from a topological

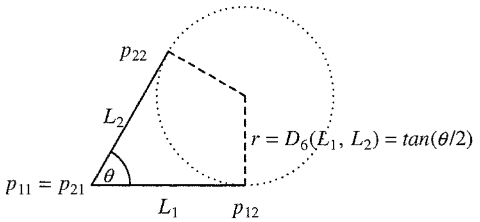

Fig. 10. The case of $D_6(L_1, L_2)$=tan(θ/2) when $|L_1|=|L_2|=1$, $p_{11}=p_{21}$ and θ= the angle between L_1 and L_2.

point of view [4] as is the case for $D_1(L_1, L_2)$ and $D_2(L_1, L_2)$. However, unlike $D_2(L_1, L_2)$, $D_5(L_1, L_2)$ fails to distinguish cases in Figs. 1(i) and (iii); this can be seen by replacing the role of the dotted circle at p''_{11} of radius $d(p''_{11}, p''_{21})$ in Fig. 1(iii) by the curve $|x''_{11} - x| + |y''_{11} - y| = |x''_{11} - x''_{21}| + |y''_{11} - y''_{21}|$, which has a diamond-shape with p''_{11} as the center and $2d(p''_{11}, p''_{21})$ being its diagonal length.

5.4. *Radius of largest circle enclosed between L_1 and L_2*

Another possible definition for the distance between two line segments is $D_6(L_1, L_2)$ = the radius of the largest circle which lies between the line segments L_1 and L_2 and which touches both L_1 and L_2 tangentially. Fig. 10 shows that $D_6(L_1, L_2) = \tan(\theta/2)$, when $|L_1| = |L_2| = 1$ and $p_{11} = p_{21}$. It follows that $D_6(L_1, L_2)$ fails to satisfy the triangle inequality when the line segments L_1, L_2, and L_3 have the same start point and the same length because "$\tan(\theta_1 + \theta_2) \leqslant \tan(\theta_1) + \tan(\theta_2)$" does not hold for all θ_1 and θ_2. Another important shortcoming of $D_6(L_1, L_2)$ is that it is not sensitive to the directions of L_1 and L_2; in particular, $D_6(L_1, L_2) = D_6(L_1^{(r)}, L_2)$ for all L_1 and L_2. Note that we cannot use the "smallest cycle" in place of the "largest cycle" above because that would violate the property (D.1).

6. Conclusion

We have presented a distance-measure between two poly-lines P_1 and P_2, given by Eqs. (7) and (8), which satisfies the five desirable properties (D.1)–(D.5). This measure is a variation of the initial measure defined by Eq. (1.1) (or Eq. (1.2)) that makes the computation of an optimal conflation transformation τ between P_1 and P_2 efficient. We have shown that many other intuitive formulations of a distance measure fail to satisfy one or more of the properties (D.1)–(D.5). We have also argued that Hausdorff's distance measure is inadequate for conflation.

Acknowledgements

The author wishes to thank Dr. Boris Kovalerchuk for suggesting the conflation-problem and to thank Anuradha Krishnan for implementing the conflation algorithm described here.

Appendix

We want to show that if both $d_1(x, y)$ and $d_2(x, y)$ satisfy the triangle inequality, then the same is true for $d(x, y) = \sqrt{d_1^2(x, y) + d_2^2(x, y)}$. Let $a_i = d_i(x, z)$, $b_i = d_i(x, y)$, and $c_i = d_i(y, z)$ so that we have $a_i \leqslant b_i + c_i$, for $i = 1, 2$. Also, let $a = d(x, z) = \sqrt{a_1^2 + a_2^2}$, $b = d(x, y) = \sqrt{b_1^2 + b_2^2}$, and $c = d(y, z) = \sqrt{c_1^2 + c_2^2}$. In order to show that $a \leqslant b + c$ holds, it suffices to show that $a_1^2 + a_2^2 = a^2 \leqslant b^2 + c^2 + 2bc = b_1^2 + b_2^2 + c_1^2 + c_2^2 + 2bc$. This holds if

$$(b_1^2 + c_1^2 + 2b_1c_1) + (b_2^2 + c_2^2 + 2b_2c_2) \leqslant b_1^2 + b_2^2 + c_1^2 + c_2^2 + 2bc,$$

i.e.,

$$b_1c_1 + b_2c_2 \leqslant bc,$$

i.e.,

$$b_1^2c_1^2 + b_2^2c_2^2 + 2b_1c_1b_2c_2 \leqslant b^2c^2 = (b_1^2 + b_2^2)(c_1^2 + c_2^2) = b_1^2c_1^2 + b_2^2c_2^2 + b_1^2c_2^2 + b_2^2c_1^2,$$

i.e.,

$$0 \leqslant (b_1c_2 - b_2c_1)^2,$$

which is clearly true and this completes the proof that $d(x, y)$ satisfies the triangle inequality.

References

[1] A. Saalfeld, Conflation: automated map compilation, Int. J. Geogr. Inf. Syst. 2 (3) (1988) 217–228.
[2] Y. Doytsher, S. Filin, E. Ezra, Transformation of datasets in a linear-based map conflation, Surv. Land Inf. Syst. 61 (2001) 159–169.
[3] S. Yuan, C. Tao, Development of conflation components, Proceedings of Geoinformatics'99 Conference, Ann Arbor, 19–21 June, 1999.
[4] S. Lang, Real Analysis, second ed., Addison-Wesley, Reading, MA, 1983.
[5] G.J. Klir, B. Yuan, Fuzzy Sets and Fuzzy Logic, Prentice-Hall, Englewood Cliffs, NJ, 1995.

About the Author—SUKHAMAY KUNDU received his PhD (Mathematics) from University of California, Berkeley and Masters (Probability and Statistics) from Indian Statistical Institute, Calcutta. His current research interests include geographic information systems, networking, and software engineering.